Title

Fetal Mouse Cardiovascular Imaging Using a High-frequency Ultrasound (30/45MHZ) System.

Author

Touma, Marlin

Publication Date

2018

DOI

10.3791/57210

Peer reviewed

Video Article

Fetal Mouse Cardiovascular Imaging Using a High-frequency Ultrasound (30/45MHZ) System

Marlin Touma[1,2]

[1]Neonatal/Congenital Heart Laboratory, Cardiovascular Research Laboratory, David Geffen School of Medicine, University of California, Los Angeles
[2]Children's Discovery and Innovation Institute, Department of Pediatrics, David Geffen School of Medicine, University of California, Los Angeles

Correspondence to: Marlin Touma at mtouma@mednet.ucla.edu

URL: https://www.jove.com/video/57210
DOI: doi:10.3791/57210

Keywords: Developmental Biology, Issue 135, Congenital Heart Defects, Genetics, Echocardiography, Fetal Circulation, Cardiac Development, Heart Maturation, Cardiovascular Physiology

Date Published: 5/5/2018

Citation: Touma, M. Fetal Mouse Cardiovascular Imaging Using a High-frequency Ultrasound (30/45MHZ) System. *J. Vis. Exp.* (135), e57210, doi:10.3791/57210 (2018).

Abstract

Congenital heart defects (CHDs) are the most common cause of childhood morbidity and early mortality. Prenatal detection of the underlying molecular mechanisms of CHDs is crucial for inventing new preventive and therapeutic strategies. Mutant mouse models are powerful tools to discover new mechanisms and environmental stress modifiers that drive cardiac development and their potential alteration in CHDs. However, efforts to establish the causality of these putative contributors have been limited to histological and molecular studies in non-survival animal experiments, in which monitoring the key physiological and hemodynamic parameters is often absent. Live imaging technology has become an essential tool to establish the etiology of CHDs. In particular, ultrasound imaging can be used prenatally without surgically exposing the fetuses, allowing maintaining their baseline physiology while monitoring the impact of environmental stress on the hemodynamic and structural aspects of cardiac chamber development. Herein, we use the High-Frequency Ultrasound (30/45) system to examine the cardiovascular system in fetal mice at E18.5 *in utero* at the baseline and in response to prenatal hypoxia exposure. We demonstrate the feasibility of the system to measure cardiac chamber size, morphology, ventricular function, fetal heart rate, and umbilical artery flow indices, and their alterations in fetal mice exposed to systemic chronic hypoxia *in utero* in real time.

Video Link

The video component of this article can be found at https://www.jove.com/video/57210/

Introduction

Congenital malformations of the heart are heterogeneous structural defects that occur during early cardiac development. Current technical advances of operational procedures have led to significant improvements in the survival rates of infants with CHDs[1,2]. However, quality of life is often compromised secondary to prolonged hospitalization and needs for staged surgical repair procedures[1,2,3,4,5]. Prenatal detection of the underlying molecular mechanisms of CHDs is crucial in order to plan early interventions, to carry out new prevention strategies, and to improve the lifelong outcomes[6,7].

Although multiple genetic and environmental factors have been implicated in CHDs pathogenesis, establishing the causality remains an unmet need to improve diagnostic, therapeutic, and preventive strategies[1,8,9,10,11,12]. Furthermore, examining the roles of *in utero* stress factors and epigenetic modifiers opens new venues for future investigations[11,12]. The last decade has indeed witnessed rapid advances in next generation sequencing technology including single nucleotide polymorphism (SNP) microarray, whole exome sequencing, and genome-wide methylation studies, their utilization in studying the genetic causes of complex human diseases, including CHDs[1,8,9,10,11] paving the way to identify novel mutations and genetic variants that have not yet been tested for their pathogenicity in suitable animal models.

Among the different disease model systems, mouse is the animal model of choice, not only for investigating mechanisms of CHDs during early cardiogenesis[13,14,15,16], but also to elucidate their impact on cardiac chamber maturation and function at late gestation in prenatal and perinatal stress factors. Hence, performing *in vivo* phenotypic characterization of a mutant fetal mouse heart, during both early and late stages of development, is crucial to understand the role of these genetic variations and environmental factors on cardiac development, and the potential future impact on chamber specific maturation processes in mice.

Early detection and accurate diagnosis of cardiac defects during development is critical for interventional planning[17,18]. Being safe, simple, portable and repeatable, fetal sonography has indeed become the standard imaging technique for cardiac evaluation in the clinic. Fetal circulation assessment using Doppler ultrasound has been widely used in clinical practice not only for the detection of cardiac defects, but also to detect vascular abnormalities, placenta insufficiency and intrauterine growth restriction, and to assess the fetal well-being in response to *in utero* insults including hypoxemia, maternal illness, and drug toxicity[17,18]. In parallel to its value in evaluating human defects and diseases, ultrasound assessment of fetal mice has gained increasing utility in experimental settings[19,20,21,22,23]. In particular, fetal heart ultrasound (echocardiography) allows sequential *in vivo* visualization of the developing heart. Many experimental studies have used ultrasound-imaging technology to observe

fetal cardiovascular development in transgenic fetal mice. Doppler ultrasound has been particularly useful to elucidate the pathophysiological parameters, such as the flow patterns in fetal circulation under physiological challenges or disease conditions[10,19]. In both humans and animals, abnormal blood flow or oxygen supply to the fetus can result from various conditions that can disrupt fetal environment *in utero* and affect the fetoplacental axis, including placental abnormalities, maternal hypoxia, gestational diabetes, and pharmaceutically induced vascular constriction[15,22]. Therefore, establishing standardized methods for performing Doppler ultrasounds on fetal mice will tremendously empower future studies of CHDs by facilitating monitoring flow patterns and key hemodynamic indices of the cardiovascular circuits during different stages of cardiac development in genetic mouse models.

High frequency ultrasound has emerged as a powerful tool to measure the developmental and physiological parameters of the cardiovascular system in mouse models and human diseases[18]. This technology has been further refined in recent years. We and other researchers have demonstrated the feasibility of this system for conducting ultra-high frequency ultrasound studies on the fetal mouse heart[15,19,20,21,22,23]. The system is equipped with Doppler color flow mapping and linear array transducers that generate two-dimensional, dynamic images at high frequency (30 to 50 MHz) frame rates. These advantages, compared to low frequency ultrasound systems and the prior generation of high frequency ultrasound[21,22], provide the necessary sensitivity and resolution for in-depth assessment of the fetal circulatory system, including comprehensive characterization of heart structures, chamber function, and flow indices of fetal mice in experimental settings. Herein, we outline methods to perform rapid assessment of cardiopulmonary circulation and feto-placental circulation at embryonic day E18.5 *in vivo* by using a high frequency system. We chose a 30/45 MHz transducer that provides an axial resolution of approximately 60 µm and a lateral resolution of 150 µm. However, a higher frequency transducer (40/50 MHz) can be chosen to analyze earlier developmental stages by following a similar methodological approach. The selected M-mode allows the visualization of tissues in motion at high temporal resolution levels (1,000 frames/s). Finally, we demonstrate the feasibility of high ultrasound for detailed comprehensive phenotypic characterization of fetal cardiovascular hemodynamic status and function in mice at baseline and in response to prenatal hypoxia stress.

Protocol

The University of California, Los Angeles, Animal Care and Use Committee has approved all procedures shown in this protocol. The experiments were conducted as part of an ongoing study under active animal protocols approved by the institutional Animal Care and Use Committee of University of California, Los Angeles, California, USA. Animal handling and care followed the standards of the Guide for the Care and Use of Laboratory Animals.

1. Preparing the High Frequency Ultrasound Imaging System

1. Turn on the ultrasound imaging system and the physiology monitoring unit.
2. Connect the 30/45 MHz transducer.
3. Place the corresponding scan head on its holder near the imaging platform.
4. Select the **Cardiac Measurement Program** option.
5. Place the ultrasound gel upside down in its pre-warming container set to 37 °C.
6. Confirm appropriate tubing system for anesthesia and verify the levels of oxygen and isoflurane.
7. Disinfect the imaging platform and the working area.
8. Set the heat level of the imaging platform to maintain constant body temperature and heart rate of the dams.

2. Pregnant Mouse Preparation

1. Place the pregnant mouse (C57/BL6) dam in the anesthesia induction chamber.
2. Induce anesthesia by using continuously delivered inhalational isoflurane (isoflurane 2%-3%) mixed with 100% oxygen (100% O_2) at a flow rate of 200 mL/min in the induction chamber.
3. Transfer the sedated animal onto the imaging platform in a supine position.
4. Provide steady-state sedation by using a facemask connected to the anesthesia tubing system-delivering isoflurane (1.0% - 1.5%) mixed with 100% O_2 at 200 mL/min.
   CAUTION: Control the leakage of anesthetic gas by using a ventilation system equipped with a charcoal filter containing canister set.
5. Tape the limbs gently to the embedded electrocardiographic electrodes after application of the electrode gel to achieve constant monitoring of maternal cardiac and respiratory rates.
6. Adjust the level of isoflurane to maintain an average heart rate of (450 +/- 50 beats/min (bpm)).
7. Maintain the body temperature within a range of 37.0 °C +/- 0.5 °C. Monitor the body temperature and heart rate being displayed on the physiology controller unit.
8. Document the vital signs of the sedated mouse every 15 min throughout the imaging procedure.
9. Assess the level of anesthesia by evaluating the mouse's posture, heart rate, and response to toe pinches.
10. Apply ophthalmic balm (1 drop into each eye) to prevent eye dryness and corneal damage.
11. Remove the fur from the mid-chest level to the lower limbs by using a depilatory cream to minimize ultrasound attenuation. Remove cream 1-1.5 min after application by alternating wet and dry gauze wipes to prevent damage to the skin.

3. Embryo Identification

1. Palpate the abdominal wall gently to locate the fetuses and spread them out.
2. Annotate each embryo on the dam's abdomen and define their anterior-posterior and dorsal-ventral orientations by using a marker.
3. Use the cervix of the sedated dam as a landmark. Label the fetuses on the left and right uterine horns as L1, L2,L 3, *etc.* (left side) and R1, R2, R3, *etc.* (right side), respectively (**Figure 1A**).

CAUTION: Avoid spreading the fetuses forcefully. 1-2 fetuses in each litter may overlap with the others, making their positioning and imaging unreliable. Exclude these fetuses from the analysis.

4. Fetal Heart Visualization and Annotation

1. Apply pre-warmed ultrasound gel on the abdomen and spread it carefully to avoid bubble formation. Add additional amount of gel on the area of scan imaging.
2. Place the ultrasound probe on its mechanical holder and mobilize it gradually towards the skin to contact with the thick gel layer while looking for the beating heart using the scanning B-Mode (**Figure 1**).
3. Click the scanning **B mode** button to obtain 2-D images. Use the bladder as a landmark to identify the first fetus positioned in the right or the left uterine horn and mark it as R1 or L1, respectively.
4. Confirm the right and left orientation of the individual fetus in real time by moving the imaging platform in the horizontal plane. Scan from head to tail to annotate the snout, the limbs, and the spine as landmarks (**Figure 1B**, Video 1).
5. Visualize the beating heart and annotate the left ventricle (LV) and the right ventricle (RV). Use color Doppler mode to optimize the heart visualization (**Figure 1 C-G**, Videos 1-2).
6. Click the scanning **B mode** button to obtain a parasternal short axis-view, have the LV and RV displayed in their maximum diameter at the center of data acquisition frame. Start live imaging (**Figure 1B-C**).
7. Change the orientation of the mouse with respect to scanning planes to obtain a longitudinal four-chamber view (**Figure 1D**). First, identify the remaining structures of the heart such as the atria, interventricular septum, and left and right outflow tracts. Next, have the ventricular and atrial chambers displayed in their maximum diameter. Then start image acquisition.
8. Exclude the non-optimal, oblique images from the final analysis. Click the **Cini** button to obtain continuous recording 'Cineloops' for a minimum of 10 s, then save the recorded images.

5. Evaluating Fetal Heart Rate and Ventricular Function

1. Click the scanning **M-mode** button to obtain cardiac images from four chamber planes (Video 3).
2. View the list of the recordings for analysis once the images of all the embryos are complete.
3. Exclude the non-optimal, oblique images from the final analysis.
4. Click the **analysis** button to measure wall thickness and the left/right ventricular internal diameter at diastole (LVID, d; RVID, d) and systole (LVID, s; RVID, s), as shown in **Figure 2**.
5. Determine the average fetal heart rate by playing each recorded M-mode tracing and calculating the measurement of one flow cycle to the following flow cycle (the spacing between adjacent peaks).
6. Perform multiple measurements (at least 5 per tracing) to obtain the average heart rate (**Figure 2**).
7. Measure the temporal changes between left ventricular internal diastolic diameter (LVID, d) and left ventricular internal diameter at end systole (LVID, s) throughout the cardiac cycle. Then calculate fractional shortening percentage (FS%) as follows: FS%=[(LVID,d-LVID,s)/LVID,d]x100.
8. Perform multiple measurements (at least 5 per tracing) to obtain the average FS% values.

6. Evaluating Cardiopulmonary Flow Parameters

1. Adjust the sector at an angle of acquisition less than 60^{o}. Click the **Doppler** Button to perform pulsed wave Doppler measurements from the 2-D four chamber-imaging plane by using a 45-MHz transducer.
    1. First, visualize the bifurcation of the pulmonary artery to identify the right outflow tract. Next, click **pulsed wave Doppler** button to obtain the flow pattern through the pulmonary and the aortic valves (**Figure 3A**, Video 4).
2. Obtain pulmonary flow measurements from pulsed wave Doppler tracing, including peak systolic velocity (PkV), acceleration time (AT), and ejection time (ET).
3. Perform multiple measurements (at least 5 per tracing) to obtain average measurements as shown in **Figure 3A** (right).
4. Calculate the AT/ET ratio for each outflow valve as an indicator of the outflow tracts patency and blood flow.
5. Proceed to obtain the mitral and aortic flow patterns from 2-D apical four chamber views using the pulsed wave Doppler. First, identify the left atrial and left ventricular chambers. Next, place the pulsed wave Doppler sample volume for recording of mitral inflow Doppler patterns and measuring early diastolic velocity (E) and atrial contraction velocity (A) (**Figure 3B**)[24,25].
6. Adjust Doppler sample volume to obtain the aortic Doppler jet pattern. Use the aortic Doppler jet tracing to measure acceleration time (AT) and ejection time (ET) as shown in **Figure 3B** (right) (Video 5)

7. Evaluating the Feto-Placental Axis

1. Use the color Doppler scan to visualize the uterine artery and feto-placental vascular tree by using the 45 MHz transducer (**Figure 4A**).
2. Identify the umbilical vessels (two arteries and one vein) in the intra-amniotic segment of the umbilical cord, just after the cord exits from the fetal abdomen.
3. Place pulsed wave Doppler sample volume to obtain the umbilical artery flow pattern (**Figure 4A**).
4. Measure vascular peak flow parameters including acceleration time (AT), ejection time (ET), and peak flow velocity at end systole (PkV, s) using the pulsed wave Doppler scanning record (**Figure 4B**).
5. Obtain 5 consecutive waveforms in each vessel, in the absence of fetal movements and maternal respiratory movements, to measure the average peak velocity for each vessel.
6. Proceed to the next embryo.

8. Post-Imaging Animal Monitoring

1. Turn off the isoflurane container following the completion of the imaging process.
2. Continue monitoring body temperature, respiratory rate, and heart rate during the recovery phase.
3. Remove the facemask and the connected tubing system once the dam starts spontaneous movements.
4. Return the dam to the appropriate housing and continue observation according to standard institutional post-procedure protocols.
5. Document the time to full resumption of normal activity.

9. Performance Requirements and Technical Considerations

1. Limit the processing time for ~8 fetuses to approximately 1 h to avoid the adverse effects of prolonged anesthesia on vital signs and physiological parameters.
2. Complete training with 8-10 pregnant mice to optimize techniques for image acquisition and flow patterns tracing in a short time frame.

Representative Results

Statistical analyses of cardiac and hemodynamic indices were performed offline. The means of 5 consecutive measurements in 3 optimal images were calculated. The data were expressed as Mean ± SEM. Student's *t*-test was used to infer intergroup comparisons. A *P* value of ≤0.05 was considered statistically significant.

Following the above protocol, we characterized the impact of chronic exposure to prenatal hypoxia on the cardiovascular status of fetal mice at late gestation by obtaining real-time high frequency ultrasound recordings on the C57/BL6 timed pregnant mice at gestational day (GD) 18.5.

After establishment of breeding groups, successful mating was confirmed. Timed pregnant dams were maintained in cages under a 12 h light-dark regime with food and water *ad libitum* until. At GD14.5, the pregnant mice were either allocated to the normoxia group (maintained in ambient air) or to the hypoxia group (placed in hypoxia chamber at 10% FiO_2 to induce systemic hypoxia). After birth, the dams and their pups remained allocated to their experimental condition until postnatal day 7 (P7).

In total, 6 dams were studied in these experiments and 42 fetuses were successfully imaged at GD18.5. Of these, data obtained from 36 fetuses were used for subsequent analysis (**Table 1**). Analysis of fetal heart rates at GD18.5 showed that hypoxic fetuses suffered from fetal bradycardia (lower heart rates) and experienced significant decline of fetal cardiac function indices (EF% and FS%) (**Table 1**). Remarkably, peak flow velocities (PkVs) of the umbilical artery PkVs were decreased in hypoxia-exposed fetuses (**Figure 4B** and **Table 1**). Furthermore, the umbilical artery acceleration time/ejection time (AT/ET) ratios revealed significantly lower values in the hypoxic compared to the normoxic fetuses, suggesting increased umbilical vascular flow resistance. In agreement, right ventricular wall thickness was increased in hypoxia-exposed fetuses as measured on 2-D/M-mode images (**Figure 5**). Since the RV assumes dominant pump function during fetal development, while the placenta serves as the primary vascular bed for oxygenation, these data collectively suggest elevated flow resistance in the feto-placental vascular circuit leading to RV hypertrophy. Importantly, hypoxia exposed newborns faced early postnatal lethality. RV failure and increased vascular resistance induced by chronic exposure to prenatal hypoxia are potentially contributing cause. Other factors, such as redox toxicity resulting from re-oxygenation injury, poor feeding, and maternal sickness cannot be excluded. Nevertheless, the exact underlying mechanism of prenatal hypoxia induced cardiac pathogenesis and the early lethality of the fetuses remain to be determined in future studies.

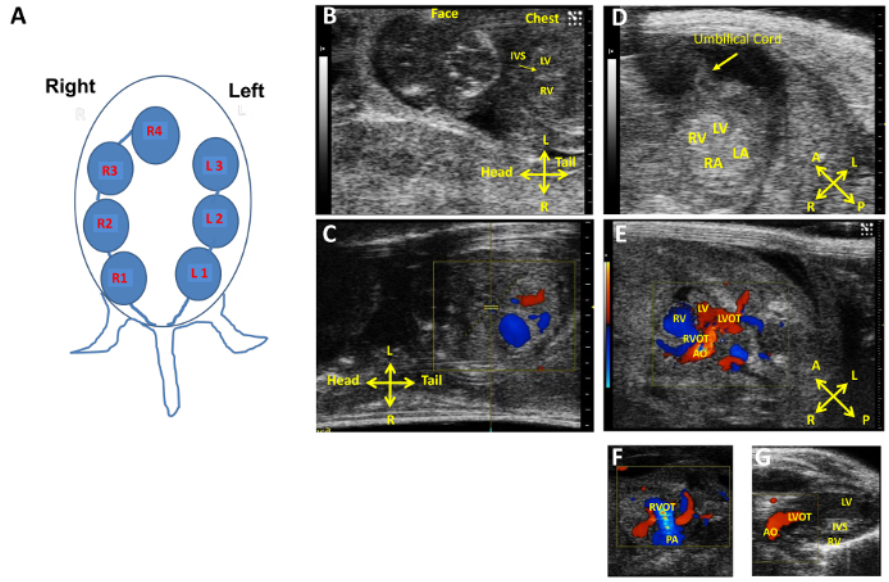

Figure 1: Fetal Mice Annotation and Heart Visualization *in Utero* Using Scanning B-Mode and Color Doppler Interrogation. (**A**) Schematic representation of fetal mice identification and annotation (L: left, R: right). (**B**) Representative image of the anatomic landmarks in a fetus to guide the orientation of gestational day 18.5 fetal heart from the parasternal short axis view of left ventricle (LV), right ventricle (RV), and interventricular septum (IVS).(**C**) Representative image of parasternal short axis view of LV and RV with color interrogation to facilitate heart chamber visualization. (**D**) Longitudinal four-chamber view of the LV and the RV, left atria (LA) and right atria (RA) color Doppler. (**E**) Longitudinal four-chamber view of LV and RV, with color Doppler interrogation to facilitate the visualization of outflow tracts: right ventricle outflow tract (RVOT), left ventricle outflow tract (LVOT), aorta (AO), and right ventricle outflow tract (RVOT). (**F**) Representative color Doppler interrogation of RVOT and PA. (**G**) Representative color Doppler interrogation of LVOT and AO. Please click here to view a larger version of this figure.

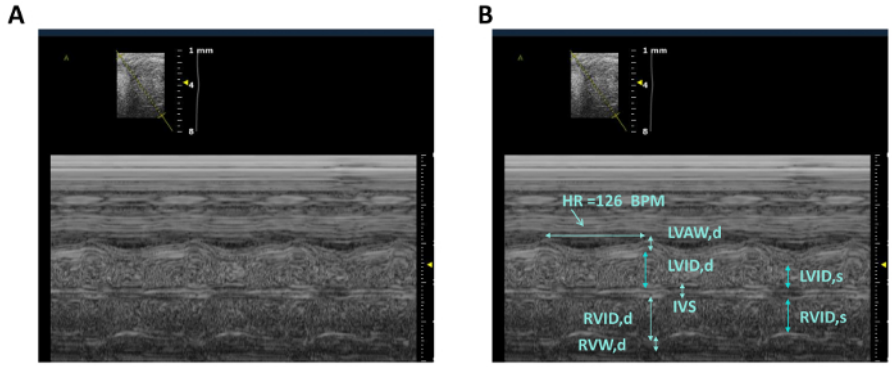

Figure 2: Assessment of Fetal Heart Rate and Ventricular Function. (**A**) Representative M-Mode tracing obtained from the long axis 4-chamber view at GD 18.5. (LV: left ventricle; RV: Right Ventricle; LA: Left Atrium; RA: right Atrium). (**B**) Representative quantification (arrowed lines) method of ventricular dimensions including left and right ventricular internal diameter at diastole (LVID, d; RVID, d) and systole (LVID, s; RVID, s), left and right ventricular wall thickness at diastole (LVAW, d; RVW, d), Interventricular septum (IVS), and beat to beat measurement of HR are shown from the four chamber imaging plane. Please click here to view a larger version of this figure.

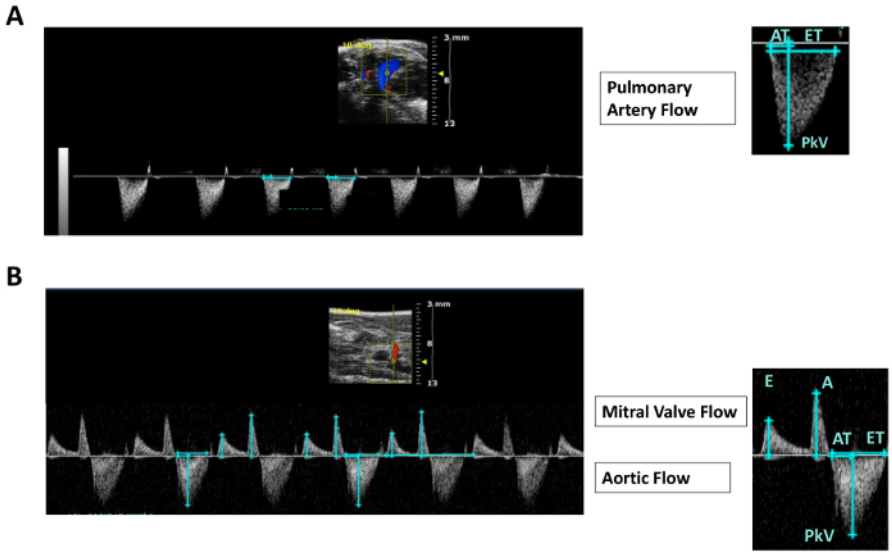

Figure 3: Pulsed Wave Doppler Tracing of Fetal Pulmonary, Aortic and Mitral Flow Indices. (**A**) Representative image of pulmonary artery pulsed wave Doppler tracing (left). Quantification methods (lines) of pulmonary flow indices PkV (peak velocity), AT (acceleration time), ET (ejection time) are shown (right) from the longitudinal four-chamber view. (**B**) Representative image of mitral and aortic pulsed Doppler flow pattern (left) and quantification of mitral valve flow indices E (early diastolic velocity) and A (atrial contraction), and aortic flow indices AT, ET, and PkV (right) are shown from the four-chamber imaging plane. Please click here to view a larger version of this figure.

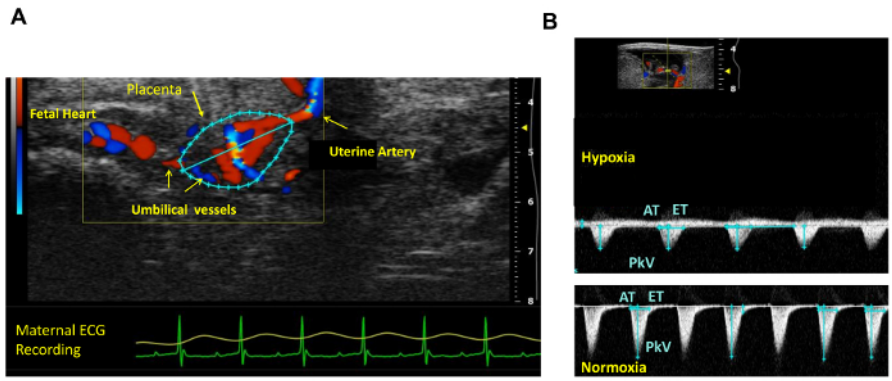

Figure 4: Assessment of Feto-placental Circulation. (**A**) Representative Image of feto-placental vascular circuits using color Doppler interrogation (upper) and maternal ECG records (lower). (**B**) Representative image of pulsed wave Doppler recording and quantification measurements (lines) of umbilical artery flow indices in hypoxia (upper) and normoxia control exposed fetal mice (Lower). PkV (peak velocity), AT (acceleration time), ET (ejection time). Please click here to view a larger version of this figure.

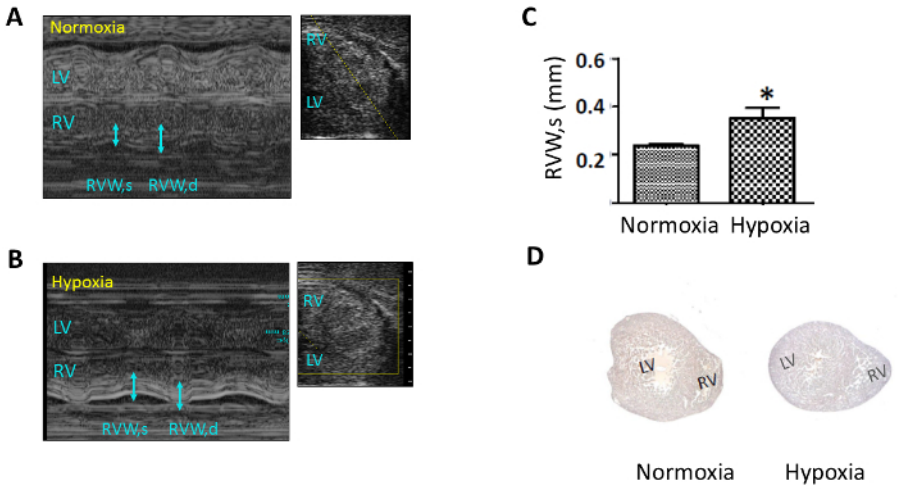

Figure 5: Assessment of Right Ventricle Wall Thickness in Hypoxia Treated Fetal Mice. (**A,B**) Representative M-Mode tracing obtained from the long axis four-chamber view at GD 18.5 in normoxia and hypoxia conditions. LV: left Ventricle, RV: right Ventricle, right ventricular wall. Lines indicate quantitative measurements of RVW thickness in systole (s) and Diastole (d). (**C**) RVW,s quantification shows increased RVW thickness in hypoxia-treated fetal mice compared to normoxia. Error Bar: Standard error of mean. (**D**) Representative cross-sectional images of fetal hearts at GD 18.5 depicting increased RV wall thickness in hypoxia treated and normoxia treated groups. Original magnification 10X. Please click here to view a larger version of this figure.

Parameter, Unit	Normoxia	Prenatal Hypoxia
Number of successfully imaged fetuses	20	16
Postnatal Mortality Rate	5%	68.75%
Hemodynamic Parameter	**(Mean ± SEM)**	**(Mean ± SEM)**
Fetal heart rate, bpm	138 ± 4	89 ± 8***
Left ventricle EF, %	71.2 ± 3	55 ± 2**
Left ventricle FS, %	43 ± 2	29 ± 4**
Pulmonary artery PkV, mm/s	102 ± 10	129 ± 8**
Pulmonary artery AT to ET ratio	0.42 ± 0.05	0.35 ± 0.03*
Umbilical artery PkV, mm/s	58 ± 4	40 ± 1.5***
Umbilical artery AT to ET ratio	0.5 ± 0.03	0.42 ± 0.025*
Umbilical vein PkV, mm/s	13 ± 1.2	19.6 ± 3**
Umbilical arterial-venous delay, ms	122 ± 4	238 ± 20*
EF, ejection fraction; FS, fractional shortening; NA, not available; NS, not significant; PkV, peak velocity; PkV, d, peak velocity during diastole; PkV, s, peak velocity during systole; Student's t test was used to infer intergroup differences. ***P <0.005. **P<0.01. *P<0.05 represents a significant difference in inter-group comparisons. student's *t-test*. Non-significance was left blank.		

Table 1: Hemodynamic parameters of normoxic and hypoxic fetal mice at gestational day 18.5. EF, ejection fraction; FS, fractional shortening; PkV, peak velocity; AT, acceleration time; ET, ejection time. Student's *t* test was used to infer intergroup differences. ****P* <0.005. ***P* <0.01, and *P<0.05 represents a significant difference in inter-group comparison.

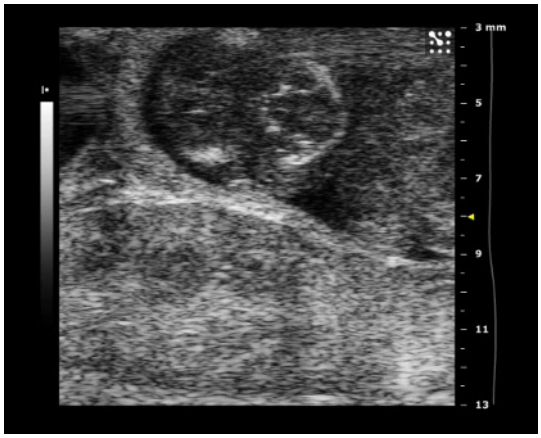

Video 1: B-mode short axis view. Please click here to view this video. (Right-click to download.)

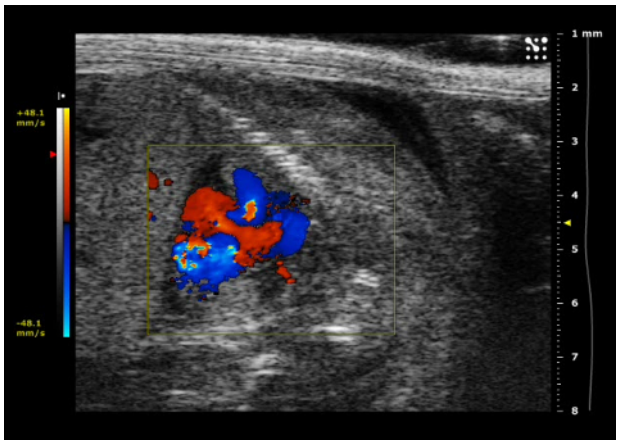

Video 2: Color Doppler – apical longitudinal view. Please click here to view this video. (Right-click to download.)

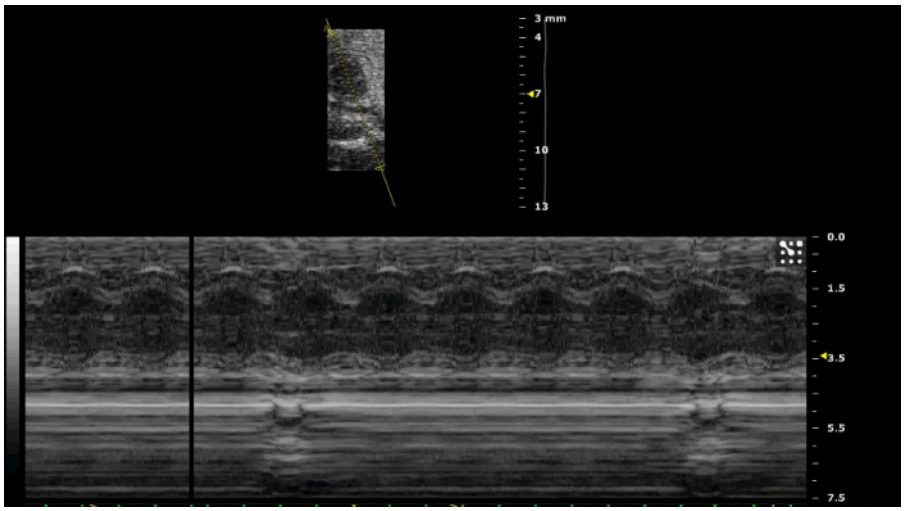

Video 3: M-Mode. Please click here to view this video. (Right-click to download.)

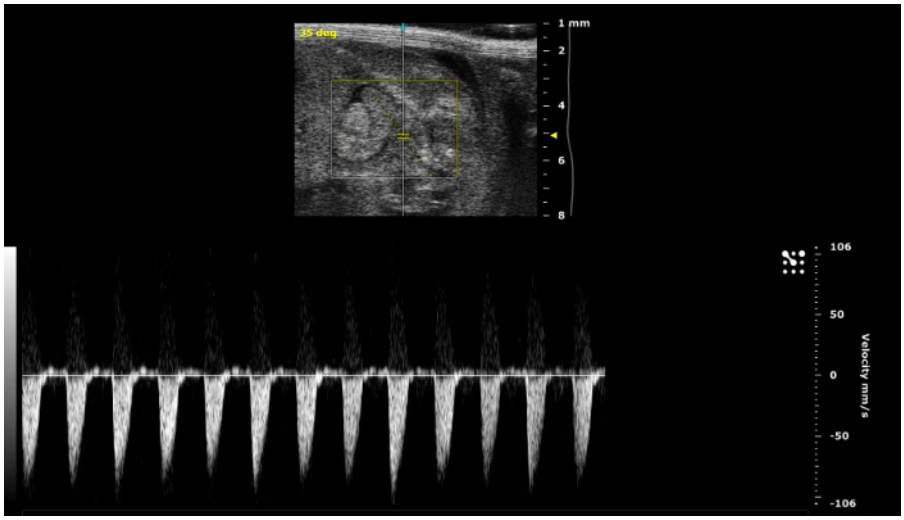

Video 4: Pulmonary artery – pulsed wave Doppler. Please click here to view this video. (Right-click to download.)

Discussion

Cardiovascular malformations and diseases are substantially influenced by genetic factors and environmental elements[19]. We have previously demonstrated a significant impact of maternal caloric restriction, initiated during the second trimester, on feto-placental circulatory flow and fetal cardiac function[9].

Prenatal hypoxia is another common stress factor during fetal development that may tremendously affect the feto-placental physiology and circulatory system. The impact of prenatal hypoxia exposure may be more profound in the context of a CHD leading to poor perinatal adaptation to postnatal life. The abnormal heart rates and cardiac indices detected in this study are indeed important indicators of cardiac stress and altered placental circulatory physiology, and thus constitute essential primary elements for detecting the developmental defects and consequent hemodynamic alterations that may become further pronounced in response to prenatal hypoxic stress leading to early heart failure. Contrary to expectations, hypoxia exposed fetuses had lower heart rates. This phenomenon may reflect immature cardiac autoregulation mechanisms in fetal mice in response to hypoxia at GD18.5. However, the exact pathogenesis remains unknown.

Although other advanced imaging methods, such as fetal cardiac MRI, allow live imaging of cardiac structures during development[20], the hemodynamic status is often lost due to static images and lengthy procedures. Noninvasive ultrasound technology, on the other hand, allows performing *in vivo* dynamic imaging that maintains the baseline physiology. Further, with the availability of high frequency transducers with enhanced resolution, the visualization of the fetal heart at different developmental stages of each individual fetus can become more feasible in transgenic mice by optimizing fetal annotation methods. Lastly, the cost per experiment is far less using this method.

In a previous report by Kim GH *et al.*, the authors provided important and novel insights regarding imaging plan optimization for data acquisition by using a prior generation of high frequency ultrasound imaging system[21]. Another report by Zhou YQ *et al.*, has established standardized baseline measurements of fetal circulation at the physiological level by using a high frequency ultrasound equipped with color Doppler system[22]. Hence, the protocol presented here complements previously established protocols, and expands to outline a comprehensive method that is feasible and practical in real time in an experimental setting. An advanced and highly sensitive high frequency ultrasound system was used in this study to scan the feto-placental circuit as a unit. The outlined protocol is simple and standardized to employ this powerful system effectively as demonstrated by achieving quantifiable measurements of hypoxia impact on fetal circulation in mice at GD18.5.

Nevertheless, we should acknowledge important limitations and challenges of fatal cardiac imaging: First, anesthetic agents, including isoflurane, may affect the physiologic parameters of the fetus. Prolonged anesthesia, hair loss, and ultrasonic gel can lead to hypothermia, which can affect the heart rate and hemodynamic indices of the dam as well as the fetuses. At present, there is no available method to evaluate the level of anesthetic agents and their impacts on the fetus. To circumvent this limitation, we titrate inhaled Isoflurane levels carefully to achieve appropriate sedation of the dams, while maintaining their basal heart rate and vital signs. Second, visualizing fetuses that are located deep in the abdomen is difficult and suboptimal, leading to exclusion of these fetuses from final data analysis. The color Doppler allows improved optimization of imaging sections and adequate alignment between the transducer and blood flow. Third, performing simultaneous analysis of all fetuses requires the operator's efficiency in rapid and accurate visualization and image acquisition rapidly, implying the importance of practical training.

Finally, key steps in this method need to be emphasized including 1) Proper preparation of the system. 2) Maintaining a stable body temperature and heart rate for the pregnant mouse. 3) Optimizing the flow rate of isoflurane to maintain baseline physiological states of the embryos to acquire reliable data. 4) Consistent and efficient image acquisition within the shortest time possible. 5) Gestational age, sex, and animal strain are important variables that may significantly affect the results. Therefore, the experimental protocol should be designed carefully to account for these variables by including matched controls from the same animal strain in data analysis and interpretation.

In conclusion, a high frequency ultrasound system is an effective method to achieve phenotypic characterization of fetal cardiovascular systems *in utero* with important experimental and scientific value and potential future applications that may include 1) Understanding the physiological dynamics during cardiac development. 2) Achieving comprehensive phenotypic analysis of genetic models of CHDs. 3) Elucidating the impact feto-placental circulation on cardiac chamber development, maturation, and adaptation to stress. 4) Performing ultrasound guided fetal injection

to study toxins, teratogens, or therapeutic agents in future. 6) Implementing the speckle tracing and strain analysis capabilities to obtain detailed regional myocardial function of the developing myocardium may provide a basis for future studies.

Disclosures

No conflict of interest declared.

Acknowledgements

We thank the animal physiology core, division of molecular medicine at UCLA for providing technical support and open access to the Vevo 2100 ultrasound biomicroscopy (UBM) system. This study was supported by the NIH/Child Health Research Center (5K12HD034610/K12), the UCLA-Children's Discovery Institute and Today and Tomorrow Children's Fund, and David Geffen School of Medicine Research Innovation award to M. Touma.

References

1. Touma, M., Reemtsen, B., Halnon, N., Alejos, J., Finn, J. P., Nelson, S. F., Wang, Y. A Path to Implement Precision Child Health Cardiovascular Medicine.*Front Cardiovasc Med.* **4**: 36 (2017).
2. Triedman, J. K., Newburger, J. W. Trends in Congenital Heart Disease. The Next Decade. *Circulation.* **133**:2716-33. (2016).
3. Gilboa, S. M., et al. Congenital Heart Defects in the United States Estimating the Magnitude of the Affected Population in 2010. *Circulation.* **134**: 101-9. (2016).
4. Pruetz, J. D., et al. Outcomes of critical congenital heart disease requiring emergent neonatal cardiac intervention. *Prenat Diagn.* **34**: 1127-32. (2014).
5. Peterson, C., et al. Hospitalizations, Costs, and Mortality among Infants with Critical Congenital Heart Disease: How Important Is Timely Detection? *Birth Defects Res A Clin Mol Teratol.* **97** (10): 664-72. (2013).
6. Atz, A. M., et al. For the Pediatric Heart Network Investigators. Prenatal Diagnosis and Risk Factors for Preoperative Death in Neonates with Single Right Ventricle and Systemic Outflow Obstruction: Screening Data from the Pediatric Heart Network Single Ventricle Reconstruction Trial. *J Thorac Cardiovasc Surg.* 140 (6): 1245-50. (2010).
7. Lalani, S. R., Belmont, J.W., Genetic Basis of Congenital Cardiovascular Malformations. *Eur J Med Genet.* 57 (8): 402-13. (2014).
8. Hanchard, N. A., Swaminathan, S., Bucasas, K., Furthner, D., Fernbach, S., Azamian, M. S., et al. A genome-wide association study of congenital cardiovascular left-sided lesions shows association with a locus on chromosome 20. *Hum Mol.* 11: 2331-41. (2016).
9. Arsenijevic, V., Davis-Dusenbery, B. N. Reproducible, Scalable Fusion Gene Detection from RNA-Seq. *Methods Mol Biol.* **1381**: 223-37 (2016).
10. LaHaye, S., Corsmeier, D., Basu, M., Bowman, J. L., Fitzgerald-Butt, S., Zender, G., et al. Utilization of Whole Exome Sequencing to Identify Causative Mutations in Familial Congenital Heart Disease. *Circ Cardiovasc Genet.* **9** (4): 320-9 (2016).
11. Zaidi, S., Choi, M., Wakimoto, H., Ma, L., Jiang, J., Overton, J. D. et al. De novo mutations in histone modifying genes in congenital heart disease. *Nature.* **498** (7453): 220-3 (2016).
12. Leirgul, E., Brodwall, K., Greve, G., Vollset, S. E., Holmstrom, H., Tell, G. S. et al. Maternal Diabetes, Birth Weight, and Neonatal Risk of Congenital Heart Defects in Norway, 1994-2009. *Obstet Gynecol.* **128** (5):1116-25 (2016).
13. Garry, D. J., Olson, E. N., A Common Progenitor at the Heart of Development. *Cell.* **127** (6):1101-4. (2006).
14. Postma, A. V., Bezzina, C. R, Christoffels, V. M. Genetics of congenital heart disease: the contribution of the noncoding regulatory genome. *J Hum Genet.* **61**: 13-9. (2016).
15. Ganguly, A., Touma, M., Thamotharan, S., De Vivo, D. C., Devaskar, S. U. Maternal Calorie Restriction Causing Uteroplacental Insufficiency Differentially Affects Mammalian Placental Glucose and Leucine Transport Molecular Mechanisms. *Endocrinology.* Oct; **157** (10): 4041-4054. (2016).
16. Lluri, G., Huang, V., Touma, M., Liu, X., Harmon, A. W., Nakano, A. Hematopoietic progenitors are required for proper development of coronary vasculature. *J Mol Cell Cardiol.* **86**: 199-207. (2015).
17. Bishop, K. C., Kuller, J. A., Boyd, B. K., Rhee, E. H., Miller, S., Barker, P. Ultrasound Examination of the Fetal Heart. *Obstet Gynecol Surv.* **72** (1): 54-61. (2017).
18. He, H., Gan, J., Qi, H. Assessing extensive cardiac echography examination for detecting foetal congenital heart defects during early and late gestation: a systematic review and meta-analysis. *Acta Cardiol.* **71** (6): 699-708. (2016).
19. Hobbs, C. A., Cleves, M. A., Karim, M. A., Zhao, W., MacLeod, S. L., Maternal Folate-Related Gene Environment Interactions and Congenital Heart Defects. *Obstet Gynecol.* **116** (2 Pt 1): 316-22. (2016).
20. Gabbay-Benziv, R., *et al.* A step-wise approach for analysis of the mouse embryonic heart using 17.6 Tesla MRI. *Magn Reson Imaging.* **35**: 46-53. (2017).
21. Kim, G. H. Murine fetal echocardiography. *J Vis Exp.* **15**; (72). pii: 4416. (2013).
22. Zhou, Y. Q., Cahill, L. S., Wong, M. D., Seed, M., Macgowan, C. K., Sled, J. G. Assessment of flow distribution in the mouse fetal circulation at late gestation by high-frequency Doppler ultrasound. *Physiol Genomics.* **46** (16):602-14. (2014).
23. Greco, A., Coda, A. R., Albanese, S., Ragucci, M., Liuzzi, R., Auletta, L., Gargiulo, S., Lamagna, F., Salvatore, M., Mancini, M. High-Frequency Ultrasound for the Study of Early Mouse Embryonic Cardiovascular System. *Reprod Sci.* **22** (12):1649-55. (2015).
24. Deneke, T., Lawo, T., von Dryander, S., Grewe, P. H., Germing, A., Gorr, E., Hubben, P., Mugge, A., Shin, D. I., Lemke, B. Non-invasive determination of the optimized atrioventricular delay in patients with implanted biventricular pacing devices. *Indian Pacing Electrophysiol J.* **10** (2):73-85. (2010).
25. Kono, M., Kisanuki, A., Ueya, N., Kubota, K., Kuwahara, E., Takasaki, K., Yuasa, T., Mizukami, N., Miyata, M., Tei, C. Left ventricular global systolic dysfunction has a significant role in the development of diastolic heart failure in patients with systemic hypertension. *Hypertens Res.* **33** (11): 1167-73. (2010).

